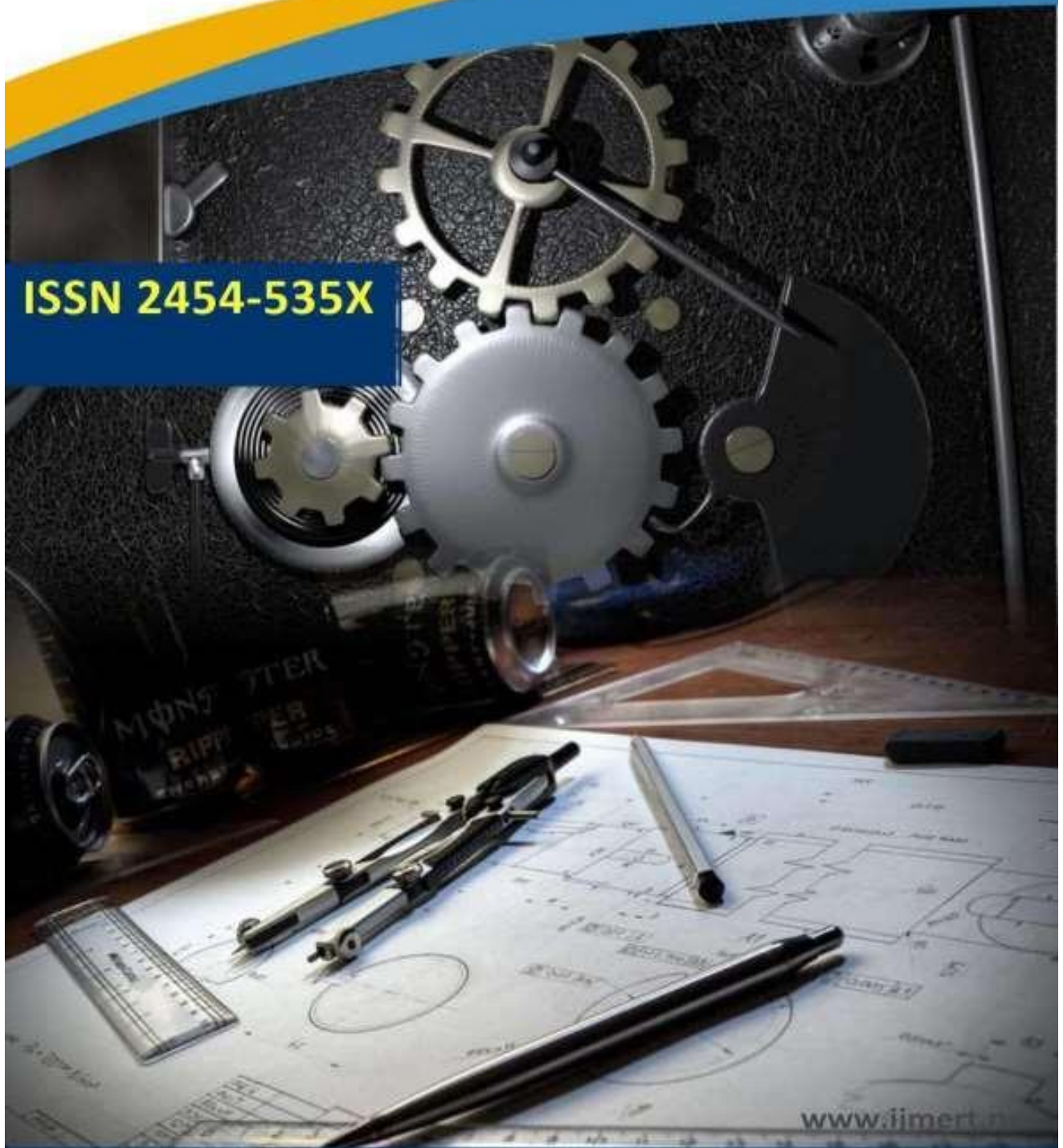




**International Journal of**  
Mechanical Engineering Research and Technology

**ISSN 2454-535X**



[www.ijmert.net](http://www.ijmert.net)

**Email ID: [info.ijmert@gmail.com](mailto:info.ijmert@gmail.com) or [editor@ijmert.net](mailto:editor@ijmert.net)**



# Immersed Boundary Method with Pressure Boundary Condition for Moving Object of Infinitesimal Thickness

**P. Sirisha \*, K. Manju, M.Sabitha, M. Sirisha & H. Hansika**

Department of Mechanophysics, Kyoto Institute of Technology, Matsugasaki, Sakyo-ku, Kyoto 606-8585, Japan

\*E-mail: [sirisha@gmail.com](mailto:sirisha@gmail.com)

**ABSTRACT:**

This study proposes and discusses the immersed boundary method (IBM) with the pressure boundary condition for flows containing moving objects of infinitesimal thickness. The pressure situation on the object border is not taken into account in the original IBM. Applying the initial IBM to the thin item results in pressure oscillations near the boundary as a result of the pressure difference between the object's front and back. The IBM with the pressure boundary condition was proposed in order to eliminate the pressure oscillations near the object boundary in the original IBM. The applicability of this method to thin objects can be improved because the IBM with the pressure boundary condition does not require the computational grid points inside the object.

KEYWORDS: immersed boundary method (IBM); oscillations; infinitesimal thickness

**INTRODUCTION**

Numerous numerical simulations of flow around objects with complex shapes in Cartesian coordinates have been carried out in recent years. Even if objects of different shapes are present in the computational domain, a new computational grid need not be created in Cartesian coordinates. When dealing with objects with complex shapes, the immersed boundary method (IBM) [1] is frequently utilized in the Cartesian grid approach. To satisfy the velocity constraint on the object boundary (virtual boundary), the forcing term is added to the momentum equations in the IBM at the grid point close to the object border. The direct forcing term estimation [2] is frequently used in the additional forcing term estimation for the IBM. When the direct forcing term estimation was used in the original IBM, the unphysical.

**IMMERSED BOUNDARY METHOD WITH PRESSURE BOUNDARY CONDITION**

Governing Equation The non-dimensional continuity equation and incompressible Navier-Stokes equations are written as,  $\frac{\partial u_{ii}}{\partial x_{ii}} = 0,$  (1)  $\frac{\partial u_{ii}}{\partial t} + u_{jj} \frac{\partial u_{ii}}{\partial x_{jj}} = F_{ii} - \frac{\partial p}{\partial x_{ii}} + G_{ii},$  (2)

$$\frac{\partial u_{ii}}{\partial t} + u_{jj} \frac{\partial u_{ii}}{\partial x_{jj}} = F_{ii} - \frac{\partial p}{\partial x_{ii}} + \frac{1}{e} \frac{\partial^2 u_{ii}}{\partial x_{jj}^2} + R_{ii} \tag{3}$$

where  $Re$  denotes the Reynolds number defined by  $Re = UL/v$ .  $U$ ,  $L$ , and  $v$  are the reference velocity, the reference length and the kinematic viscosity, respectively. The last term of Eq. (2),  $G_{ii}$ , denotes the additional forcing term for the IBM.  $F_{ii}$  denotes the convective and diffusion terms.

**Numerical Method**

The incompressible Navier-Stokes equations (2) are solved by the second order finite difference method on the collocated grid arrangement. The convective terms are discretized by the second order fully conservative finite difference method [7]. The diffusion and pressure terms discretized by the usual second order centered finite difference method. For the time integration, the fractional step approach [8] based on forward Euler method is applied.

For the incompressible Navier-Stokes equations in the IBM, the fractional step approach can be written by

$$u_{ii}^* = u_{ii}^* + \Delta t F_{ii}^n, \tag{4}$$

$$u_{ii}^{n+1} = u_{ii}^* + \Delta t \left( -\frac{\partial \partial p^n}{\partial x_{ii}} + G_{ii} \phi \right), \tag{5}$$

where  $u_{ii}^*$  denotes the fractional step velocity and  $\Delta t$  is the time increment. The resulting pressure equation is solved by the SOR method. In this paper, The convergence criterion of the momentum equations and pressure equation is set as  $\phi_{\phi_{12}} < 1.0 \times 10^{-6}$ , where  $\phi_{\phi_{12}}$  is the L-2 residual of physical quantities  $\phi\phi$ , i.e., the velocity or pressure.

**Forcing Term Estimation**

In order to estimate the additional forcing term in the governing equations,  $G_{ii}$ , there are mainly two ways, that is, the feedback [9] [10] and direct [2] forcing term estimations. In this paper, the direct forcing term estimation in Fig 1 is adopted. For the forward Euler time integration, the forcing term can be determined by

$$G_{ii} = -F_{ii}^n + \frac{\partial \partial p^n}{\partial x_{ii}} + \frac{\phi_{ii}^{n+1} - u_{ii}^n}{\Delta t}, \tag{6}$$

where  $\phi_{ii}^{n+1}$  denotes the interpolated velocity by linear interpolation. Namely, the forcing term is specified as the velocity components at next time step satisfy the relation,  $\phi_{ii}^{n+1} = u_{ii}^{n+1}$ . In this forcing term estimation for the original IBM, the grid points added the forcing term are restricted near the virtual boundary. Then, the pressure distributions near the virtual boundary show unphysical oscillations.

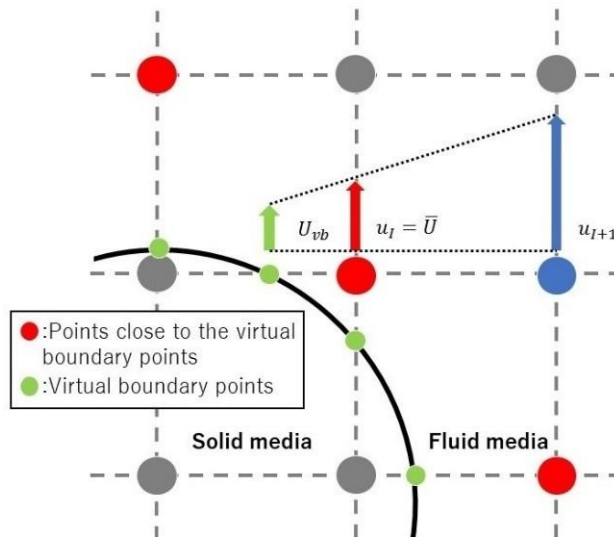


**Figure 1.** Direct forcing term estimation Pressure Boundary Condition on Virtual Boundary In the present IBM, the pressure condition on the virtual boundary ( $\frac{\partial p}{\partial n} = 0$ ) is considered. When the grid point

on the front side of the plate is  $(I, J)$  as Fig. 2, the pressure gradient in the  $x$  direction is written as

$$\frac{\partial p}{\partial x} \Big|_{I,J} = \frac{p_{I+1,J} - p_{I-1,J}}{2\Delta x}, \tag{7}$$

where  $\hat{p}_{I+1,J}$  denotes the pressure that satisfies the pressure condition on the virtual boundary. If the virtual boundary is arranged along the grid points, the formula  $\hat{p}_{I+1,J} = p_{I,J}$  is completed. Otherwise,  $\hat{p}_{I+1,J}$  is estimated from the pressure at surrounding grid points and the boundary conditions on the virtual boundary. [11].

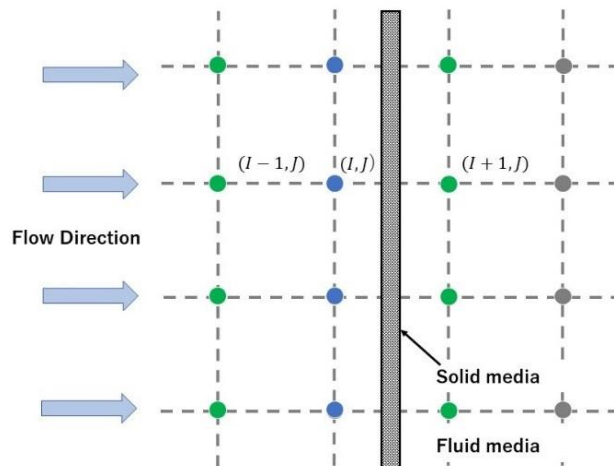


**Figure 2.** Grid points where the pressure condition is considered

**FLOW AROUND A PLATE OF INFINITESIMAL THICKNESS**

In order to validate the effectiveness of the present IBM, the flow around the moving plate

of infinitesimal thickness is considered. The present IBM is compared to the original IBM

and the boundary-fitted grid approach (BFG). The computational domain is shown in Fig3. In order to reduce the number of grid points, the hierarchical Cartesian grid with level 2 is introduced. The grid resolution near the plate is  $\Delta x = \Delta y = 0.025D$ , where  $D$  is the plate length. In this paper, the plate length is set as  $D = 1$ . The time increment is  $\Delta t = 0.001$ , the analysis is performed to non-

dimensional time  $t = 100$ . The plate is placed vertically and the initial position of the plate center is  $(x_0, y_0) = (8.0D, 5.5D)$ . The plate is stationary until  $t = 10$ , and moves to negative  $x$  direction from  $t = 10$  at the velocity of  $U_{plate} = 0.25D$ , and the plate stops at  $(x_0, y_0) = (4.0D, 5.5D)$ . So the moving velocity of the plate is written as Eq. (8).

$$U_{plate}(t) = \begin{cases} 0.00D & (0 \leq t < 10) \\ 0.25D & (10 \leq t < 26) \\ 0.00D & (26 \leq t < 100) \end{cases} \quad (8)$$

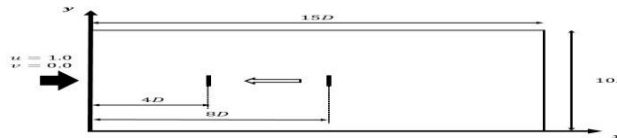
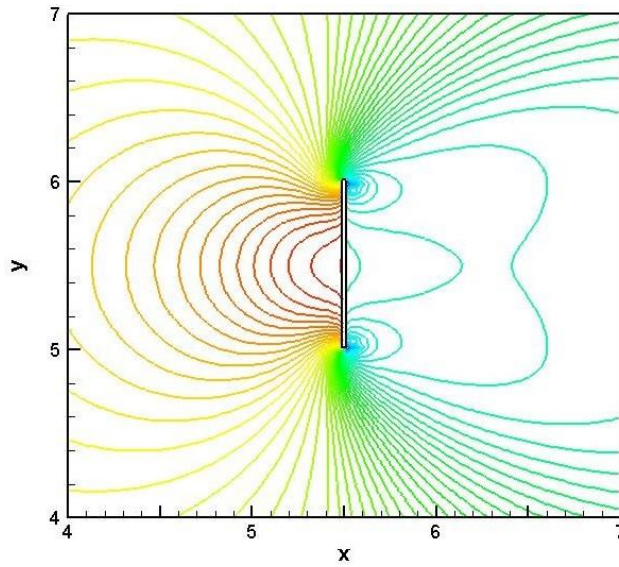


Figure 3. Computational domain for the moving plate of infinitesimal thickness

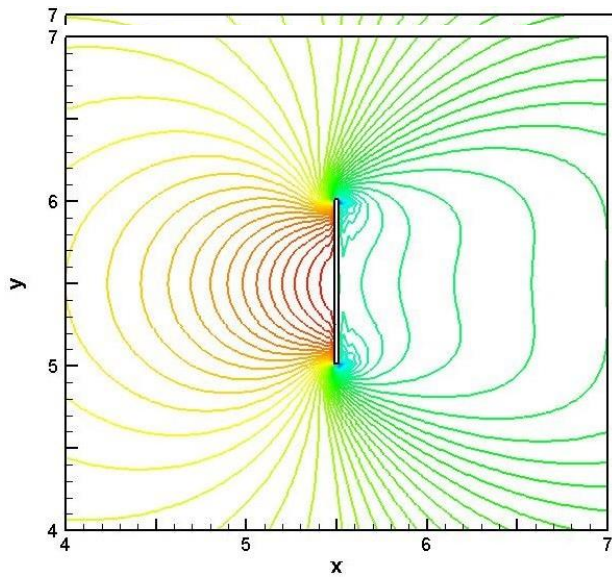
The impulsive start determined by the uniform flow ( $u = 1, v = 0, p = 1$ ) is adopted. On the inflow boundary (left boundary), the velocity is fixed by the uniform flow, and the pressure is imposed by the Neumann condition obtained by normal momentum equation. On the outflow boundaries (right, top and bottom boundaries), the velocity is extrapolated from the inner points and the pressure is obtained by the Sommerfeld radiation condition [12]. On the virtual boundary, the velocity condition is the nonslip ( $u = U_{plate}, v = 0$ ) condition. The Reynolds number is set as  $Re = 40$ . Note that the flow around the stationary plate which is equivalent to the above conditions is handled in the BFG. In this case, the plate is always stationary at  $(x_0, y_0) = (5.5D, 5.5D)$ , and on the inflow boundary, the velocity is fixed by the uniform flow ( $u = 1.25, v = 0$ ). Other conditions are the same as the cases of the present IBM and the original IBM. In this paper, analysis by each approach is described as

- Case-1. BFG,
- Case-2. Original IBM,
- Case-3. Present IBM.

Figures 4, 5 show the pressure contours around the plate at  $t = 20, 25$ . The center of the plate is located at  $(x_0, y_0) = (5.5D, 5.5D), (4.25D, 5.5D)$  respectively at each time. Figure 6 shows the pressure distributions on the center of the flow at  $t = 20$ . As can be seen from Figs. 4-6, the unphysical pressure oscillations appear in Case-2. By contrast, in Case-3, the pressure oscillations are suppressed and relatively smooth pressure distributions are obtained. However, the pressure distributions behind the plate in Case-2 and 3 are different from that in Case-1.



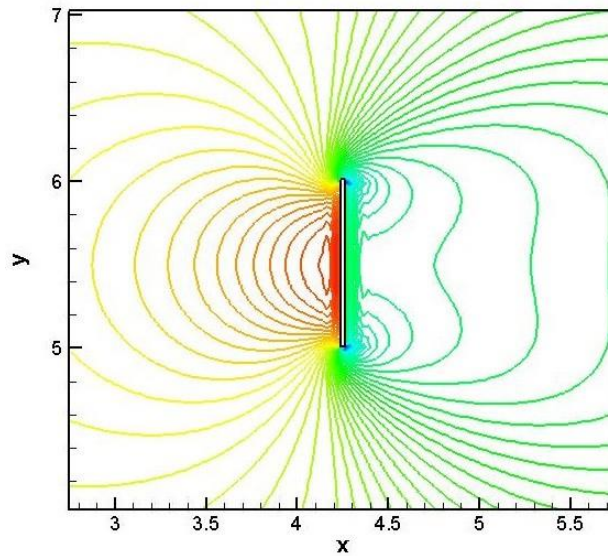
(a) Case-1



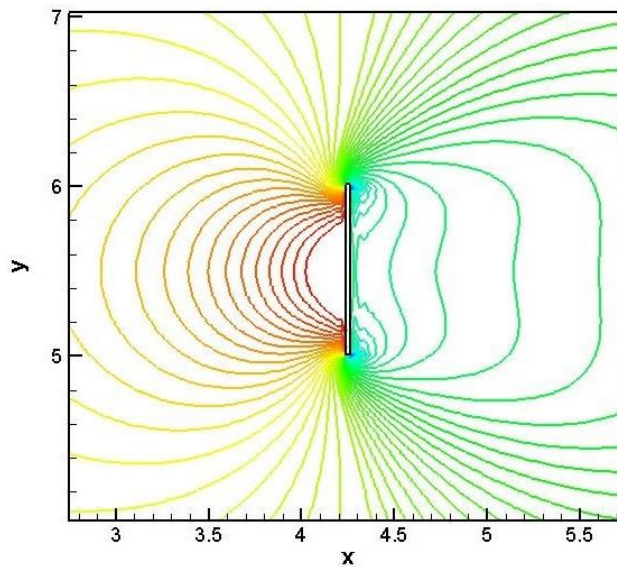
(b) Case-2

(c) Case-3

**Figure 4.** Pressure contour around the plate at  $t = 20$   
(Case-1, Case-2 and Case-3)

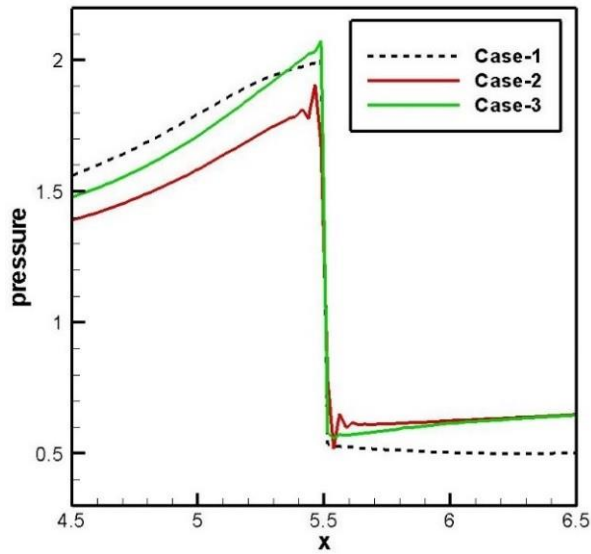


(a) Case-2

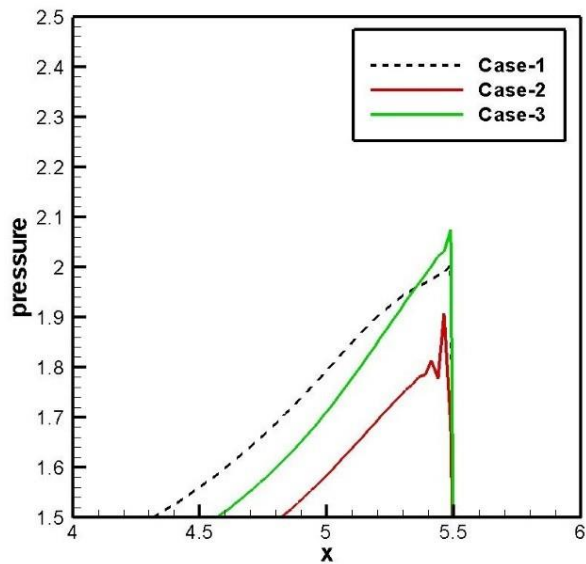


(b) Case-3

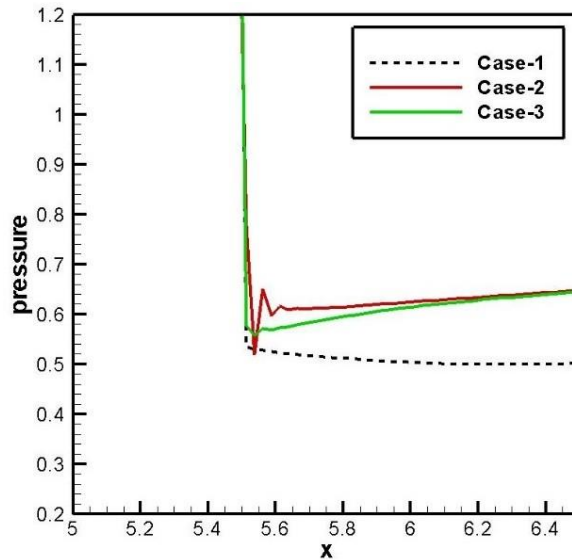
**Figure 5.** Pressure contour around the plate at  $t = 25$   
(Case-2 and Case-3)



(a) overall view



(b) front of the plate



(c) behind of the plate

**Figure 6.** Pressure distribution on the center of the flow at  $t = 20$  (Case-1, Case-2 and Case-3)

Figure 7 shows the time history of the drag coefficient around  $t = 20$ . In this paper, the drag coefficient is estimated by

$$C_D = \frac{\int_b p_x ds + \int_b r_x ds}{\frac{1}{2} \rho_0 U_0^2 S}, \tag{9}$$

where  $b$  denotes the virtual boundary,  $p_x$  and  $r_x$  is the  $x$  direction components of the interpolated pressure and shear stress on the surface of the plate.  $\rho_0$  and  $U_0$  denote the reference density and velocity of the flow. In this paper, the plate placed vertically, therefore it is  $r_x = 0$ . From Fig. 7, the drag coefficients are not stable in Case-2 and Case-3. This is because the forcing points change by moving the virtual boundary beyond the computational grid. This influence is particularly noticeable in Case-3 where the pressure condition on the virtual boundary is considered. However, the drag coefficient in Case-3 is closer to the it in Case-1 than in Case-2. Therefore, the effectiveness of the present method can be confirmed.

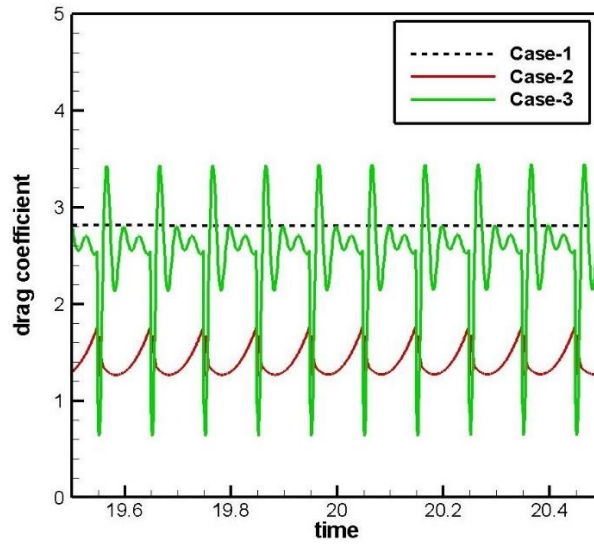


**Figure 7.** Time history of the drag coefficient around  $t = 20$  (Case-1, Case-2 and Case-3)

Application to Overset Grid System

In the previous section, it could be confirmed that the pressure oscillations near the virtual boundary of the moving plate are suppressed by the present IBM. In this session, the present method is combined with the overset grid system [13, 14] in order to reduce the influence by moving the virtual boundary beyond the computational grid in IBM. The Navier-Stokes equations are rewritten

$$\frac{\partial u_i}{\partial t} = F_i - \frac{\partial p}{\partial x_i} + G_i \tag{10}$$

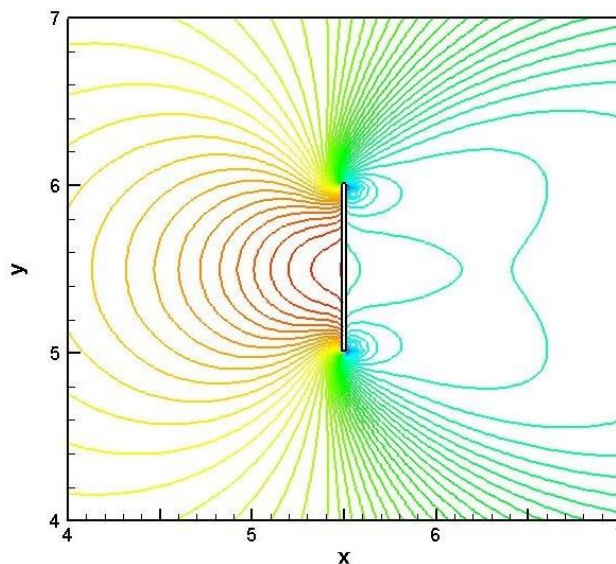
$$\frac{\partial u_i}{\partial x_j} = \frac{1}{Re} \frac{\partial^2 u_i}{\partial x_j^2} \tag{11}$$

$$F_i = -\rho u_{jj} - c_{jj} \frac{\partial u_i}{\partial x_j} + \frac{1}{Re} \frac{\partial^2 u_i}{\partial x_j^2}$$

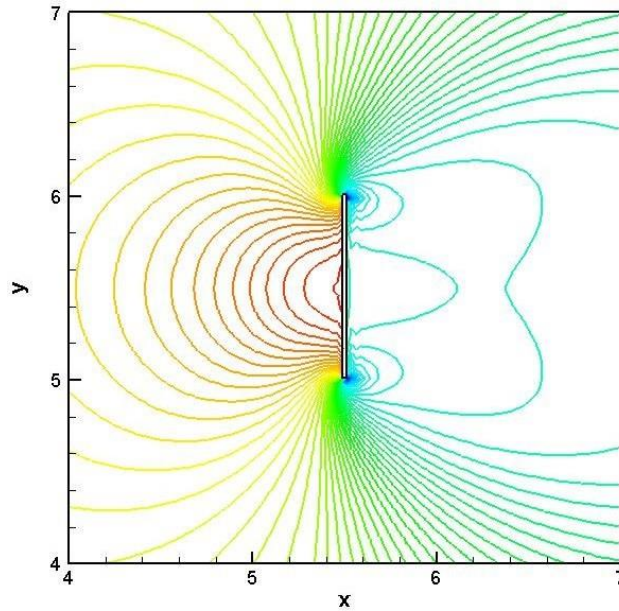
based on the ALE formulation. Where,  $c_{jj}$  is the moving velocity component of the computational grid for the ALE method. In the overset grid system,  $c_{jj} = 0$  at the main-grid because the ALE method is only applied to the sub-grid.

In order to verify the present method combined with the overset grid system, the same flow analysis as the previous session is performed (Case 4). In this flow analysis, the sub-grid follows the moving plate, i.e.  $c_x = U_{plate}$ .

Figure 8 shows the pressure contours around the plate at  $t = 20$ . The center of the plate is located at  $(x_0, y_0) = (5.5D, 5.5D)$ . Figure 9 shows the pressure distribution on the center of the flow at  $t = 20$ . As can be seen from Figs. 8, 9, the pressure distribution behind the plate of Case-4 is in good agreement with the reference result [15-18].



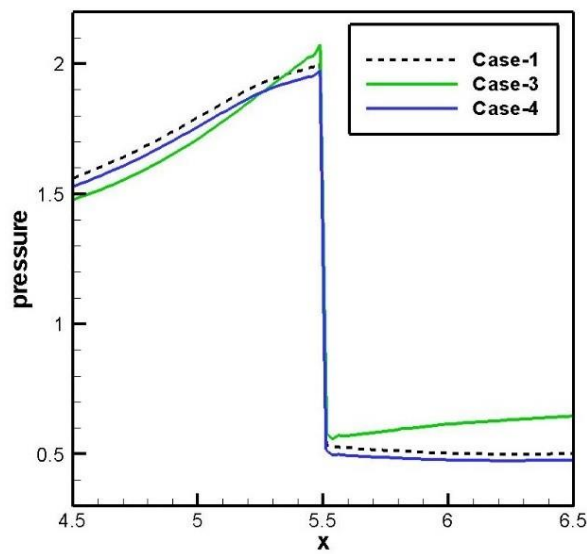
(a) Case-1



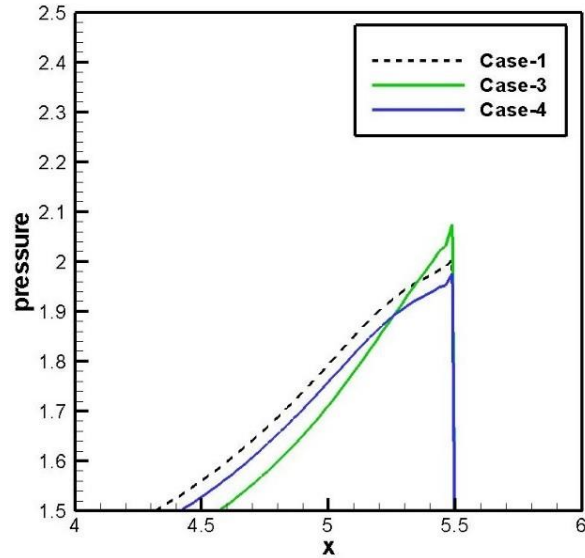
(b) Case-4

**Figure 8.** Pressure contour around the plate at  $t = 20$

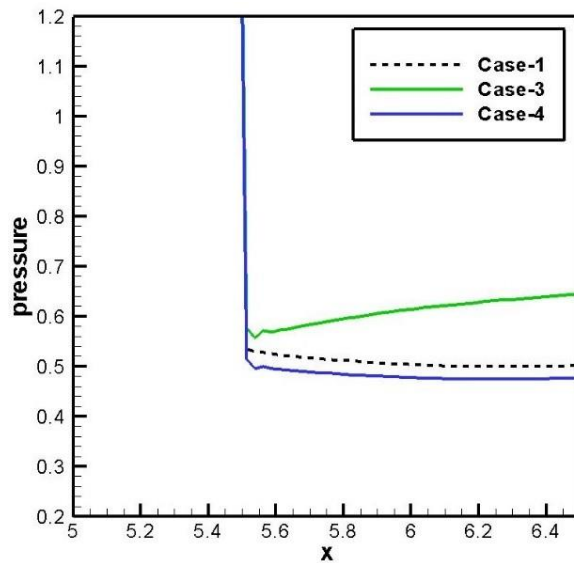
(Case-1 and Case-4)



(a) overall view



(b) front of the plate



(c) behind of the plate

**Figure 9.** Pressure distribution on the center of the flow at  $t = 20$  (Case-1, Case-3 and Case-4)

Figure 10 shows the time history of the drag coefficient around  $t = 20$ . In Fig. 10, the oscillations of the drag coefficient that appeared in Case-3 are dramatically suppressed in Case-4. The drag coefficients at  $t = 20$  are  $C_D = 2.808$  and  $2.692$  obtained by Case-1 and Case-4 respectively, and the error was 4.13%. From these results, it is concluded that the present method combined with the overset grid system is effective for the flow analysis including the moving plate of infinitesimal thickness.

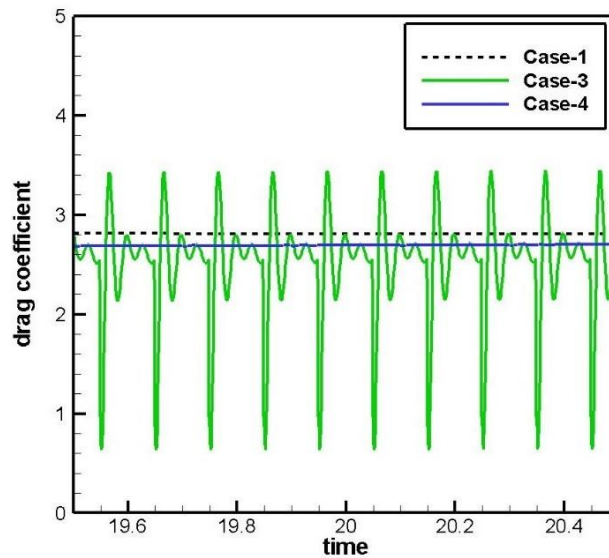


**Figure 10.** Time history of the drag coefficient around  $t = 20$  (Case-1, Case-3 and Case-4)

**CONCLUSIONS**

In this study, the IBM with the pressure condition was applied to a moving plate of infinitesimal thickness object and its effectiveness was verified. The results obtained by the present IBM are compared to the results obtained by the original IBM and the BFG approach. As a result, it is concluded that the present IBM is effective in suppressing the pressure oscillations near the virtual boundary that appeared in the original IBM. However, in the present and original IBM, the oscillations of the time history of the drag coefficients appeared because the forcing points change by

moving the virtual boundary beyond the computational grid. In order to reduce the influence by moving the virtual boundary beyond the computational grid in IBMs, we proposed a method combining the IBM with pressure condition and the overset grid system. As a result, the oscillations of the drag coefficient were removed, and the pressure distributions around the plate were in good agreement with the reference result. From these results, we conclude that the present IBM combined with the overset grid system is effective for the analysis of the flow including the moving object of infinitesimal thickness.

**REFERENCES**

[1] C.S. Peskin, D.M. McQueen. “A three-dimensional computational method for blood flow in the heart I. Immersed elastic fibers in a viscous incompressible fluid”. *Journal of Computational Physics*, Vol. 81, no.2, pp. 372-405, 1989.

[2] E.A. Fadlun, R. Verzicco, P. Orlandi, J. Mohd-Yosof. “Combined immersed-boundary finite-difference methods for three-dimensional complex simulations”. *Journal of Computational Physics*, vol.

161, no. 1, pp. 35–60.

[3] H. Nishida, K. Sasao, “Incompressible Flow Simulations Using Virtual Boundary Method with New Direct Forcing Terms Estimation”. *Proceedings of International Conference on Computational Fluid Dynamics 2006*, pp. 185–186, 2006.

[4] H. Kagomi, M. Tanaka, K. Tajiri, H. Nishida, “Study on flow around butterfly-like flapping model using ALE seamless immersed boundary method”. *Proceedings of the 31st symposium on computational*



- fluid dynamics*, pp. 1-4, 2017. (Japanese)
- [5] K. Tajiri, H. Nishida, M. Tanaka. “Numerical Simulation of Incompressible Flows using Immersed Boundary Method Considering the Pressure Condition”. *Ninth International Conference on Computational Fluid Dynamics*, vol. 126, pp. 1-12, 2006.
- [6] K. Tajiri, H. Nishida, M. Tanaka. “Comparison of Handling Pressure in Poisson Solver for Immersed Boundary Method Considering Pressure Condition,” *Procedia Computer Science*, vol. 108, pp. 1933- 1942, 2017.
- [7] M.Y. Ali, K.R. Chowdhury, A. Sultana, N.K. Mitra. “Studies on Soft Hemirings And Its Application In Graph Theory”. *Matriks Sains Matematik*, vol. 2, no. 2, pp. 32-36, 2018.
- [8] M. Elmnifi, M. Alshilmany, M. Abdraba. “Potential of Municipal Solid Waste in Libya For Energy Utilization”. *Acta Mechanica Malaysia*, vol. 2, no. 1, pp. 11-15, 2019.
- [9] D.Y. Xu. “Research on Supply Chain Management Strategy of Longtang Electric Engineering Co. Ltd”. *Acta Electronica Malaysia*, vol. 3, no. 1, pp. 10-13, 2019.
- [10] W. Tianlei. “Nonlinear Control Strategies and Planning for Underactuated Overhead Cranes”. *Engineering Heritage Journal*, vol. 3, no. 1, pp. 09-12, 2019.
- [11] Y. Morinishi, T.S. Lund, O.V. Vasilyev, P. Moin. “Fully conservative higher order finite difference schemes for incompressible flow”. *J. Comput. Phys*, vol. 143, no. 90, pp. 90-124, 1998.
- [12] C.M. Rhie, W.L. Chow. “Numerical Study of the Turbulent Flow Past an Airfoil with Trailing Edge Separation”. *AIAA journal*, Vol. 21, no. 11, pp. 1525-1532, 1983.
- [13] D. Goldstein, R. Handler, L. Sirovich. “Modeling a no-slip flow boundary with an external force field”. *Journal of Computational Physics*, vol. 105, no. 2, pp. 354–366, 1993.
- [14] E.M. Saiki, S. Biringen. “Numerical simulation of a cylinder in uniform flow: application of a virtual boundary method”. *Journal of Computational Physics*, vol. 123, no. 2, pp. 450–465, 1996.
- [15] H. Nishida. “Development of Seamless Immersed Boundary Method to Various Partial Differential Equations”. *Proceedings of Korea-Japan CFD Workshop 2015*, pp. 1-15, 2015.
- [16] K. Kawakami, H. Nishida, N. Satofuka. “An open boundary condition for the numerical analysis of unsteady incompressible flow using the vorticity-stream function formulation”. *Transactions of the Japan Society of Mechanical Engineers Series B*, vol. 60, no. 574, pp. 1891–1896, 1994. (Japanese)
- [17] J.A. Benek, P.G. Buning, J.L. Steger. “A 3-D chimera grid embedding technique”. *AIAA Paper*, pp. 85- 1523, 1985.
- [18] K. Tajiri, H. Nishida, M. Tanaka, “Large Eddy Simulation of Turbulent Flow using Seamless Immersed Boundary Method”. *Proceedings of 8th International Conference on Computational Fluid Dynamics*, Vol.0197, pp. 1–13, 2014.